

The use of Geant4 for simulations of a plastic β -detector and its application to efficiency calibration

V.V. Golovko^{a,1} V. E. Jacob^a J. C. Hardy^a

^a*Cyclotron Institute, Texas A&M University, College Station, TX 77843-3366, USA*

Abstract

Precise β -branching-ratio measurements are required in order to determine ft -values as part of our program to test the Electroweak Standard Model via unitarity of the Cabibbo-Kobayashi-Moskawa matrix. For the measurements to be useful in this test, their precision must be close to 0.1%. In a branching-ratio measurement, we position the radioactive sample between a thin plastic scintillator used to detect β -particles, and a HPGe detector for γ -rays. Both β singles and β - γ coincidences are recorded. Although the branching ratio depends most strongly on the HPGe detector efficiency, it has some sensitivity to the energy dependence of the β -detector efficiency. We report here on a study of our β -detector response function, which used Monte Carlo calculations performed by the Geant4 toolkit. Results of the simulations are compared to measured β -spectra from several standard β -sources.

Key words: Precise β -branching-ratio measurements; the Electroweak Standard Model; unitarity of the Cabibbo-Kobayashi-Moskawa matrix; Monte Carlo simulations; Geant4 efficiency calculation for plastic β -detector.

1. Introduction

Knowledge of the total efficiency of a plastic β -detector is crucial to our precision experiments testing the Electroweak Standard Model. We measure the ft values for superallowed $0^+ \rightarrow 0^+$ nuclear transitions, from which we obtain the value of V_{ud} , the up-down quark-mixing element of the Cabibbo-Kobayashi-Moskawa (CKM) matrix. This requires that half-lives, branching ratios and decay energies all be measured with high precision, 0.1% or better. (The most recent complete review of this work can be found in Ref. [1], with an update in Ref. [2]). Since branching ratios are typically determined from the intensities of β -delayed γ rays that are observed in β - γ coincidence measurements, it is the γ -

ray detector's efficiency that is most crucial in aiming for 0.1% precision. However, a good knowledge of the energy-dependence of the β -detector's efficiency is also required. Here we report studies of our β -detector's response function, with source measurements and Monte Carlo calculations performed with the Geant4 (version 4.9.0) toolkit [3].

In a typical measurement of a β -decay branching ratio (see, for example, Ref. [4,5]), we implant a radioactive species into Mylar tape, then rapidly move the tape to a shielded counting station, where the sample is positioned between a 1-mm-thick plastic scintillator to detect β -particles, and a 70% HPGe detector to detect γ -rays. We record both β singles and β - γ coincident events. Since the efficiency of the HPGe detector has been very precisely determined [6], to first order a β -branching ratio is simply given by the measured number of coincident γ rays that follow that β branch divided by the total number of β singles from all branches; the β -detector

Email address: vgolovko@comp.tamu.edu (V.V. Golovko).

¹ This work was supported by the U.S. Department of Energy under Grant No. DE-FG03-93ER40773 and by the Robert A. Welch Foundation under Grant No. A-1397.

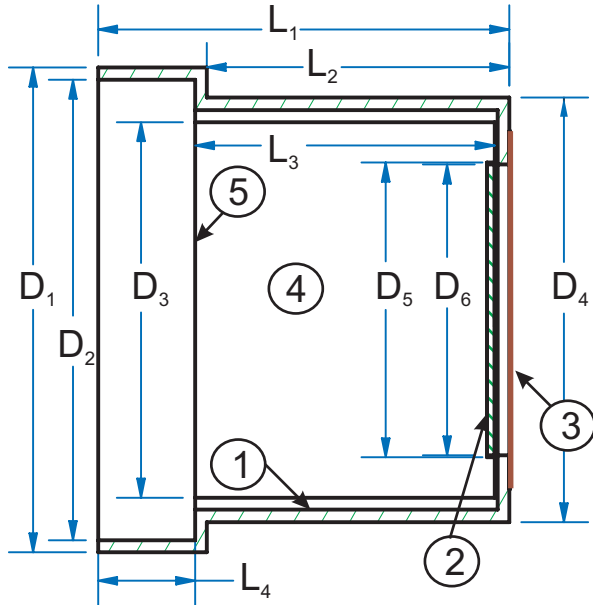


Fig. 1. Schematic drawing of the β -detector. Labeled dimensions are given in Table 1; others appear in the text. Incident β -particles from a radioactive source pass through a thin havar-foil window (3) and into the plastic-scintillator disc (2). The disc is recessed into a lucite light guide (4), which is coupled to a phototube (not shown in the figure) at surface 5. The scintillator and light guide are enclosed in a cylindrical cover (1) made from PVC.

efficiency simply cancels out and need not be determined. For high precision, though, it becomes necessary to account for the slightly different efficiency of the β detector for each β transition, a difference that affects the measured intensities of the coincident γ rays.

The energy dependence of our β -detection efficiency is caused principally by the low-energy electronic threshold, which removes a slightly different fraction of the total β spectrum for different end-point energies. Since our threshold is at ~ 80 keV and, for our superallowed-decay studies, end-point energies are typically 2 MeV or more, we lose at most a few percent of the total β particles for any single transition. Thus the change in this loss from transition to transition in the same decay is even smaller. Nevertheless, the precision we strive for in our branching-ratio measurements is very high and we seek to account reliably for that energy dependence. Even though a Monte Carlo code like Geant4 should be well suited to simulating the response function of a thin plastic scintillator, we considered it important to test and evaluate the code's results first, by comparing them against experimental data taken with several β sources that also emit

conversion-electrons: ^{133}Ba , ^{137}Cs and ^{207}Bi .

The Geant4 toolkit used in treating the transportation of β and γ particles through matter is both modular and flexible, especially in the description of low-energy electromagnetic processes down to 250 eV (see, for example Ref. [7,8]). In addition, it is also possible to simulate rather complicated 3-D geometry, select a variety of materials and decay products (including radioactive ions), and choose how to handle the physical processes governing particle interactions. Moreover, it provides output of the simulated data at different stages in the calculation and under various selection criteria. An overview of recent developments in diverse areas of this toolkit is presented in Ref. [9].

2. Detector Arrangement and Measurements

The β -detector assembly is illustrated in Fig. 1, with detailed dimensions given in Table 1. It consists of a 1-mm-thick Bicorn BC404 scintillator disc recessed into a cylindrical Lucite light guide, to which it is optically coupled. The light guide, in turn, is optically coupled to a photomultiplier tube (not shown in the figure and not included in the simulations). Optical cement (BC-600) from Bicorn was applied to the surfaces between the scintillator and the light guide, and between the light guide and the photomultiplier tube (R329P from Hamamatsu). The scintillator disc, light guide and the last 13 mm of the phototube are enclosed in an opaque cylindrical shield made from 1.5-mm-thick polyvinyl chloride (PVC). The opening in the scintillator end of

Table 1
Measured detector dimensions used in our Monte Carlo calculations. Letters in the second column correspond to labels in Fig. 1.

Detector parameter		Value (mm)
Outer shoulder, ϕ	D ₁	63.50
Inner shoulder, ϕ	D ₂	60.33
Light guide, ϕ	D ₃	49.20
Outer PVC cover, ϕ	D ₄	55.63
Hole in PVC cover, ϕ	D ₅	38.61
Plastic scintillator, ϕ	D ₆	38.10
Length of PVC cover	L ₁	53.85
Length of outer shoulder	L ₂	39.62
Length of light guide	L ₃	39.24
Length of inner shoulder	L ₄	12.70

the PVC shield is slightly larger in diameter than the scintillator disc, and is covered with a pin-hole-free, 5- μm -thick havar foil. The β -particles enter the detector assembly through this foil with essentially negligible energy loss.

For our measurements of the detector response function, each radioactive source was placed at a distance of 13 mm from the havar window of the detector assembly and was axially aligned with it. The distance was determined with the aid of an AccuRange 600TM Laser Displacement Sensor (model AR600-4000) [10], which measures distance with an absolute precision better than 0.1 mm. Both detector and source were placed on stands on a lab table (in air at atmospheric pressure) as far away as possible from other objects. We used three different 37-kBq sources – ^{133}Ba , ^{137}Cs and ^{207}Bi . All three were open sources sold by Isotope Products Laboratories as “conversion electron sources.” Each source, being specially prepared to minimize scattering or degradation of the emitted electrons, had been deposited as a 5-mm-diameter spot on a thin foil – stainless steel with a thickness of 51 μm in the case of ^{207}Bi , aluminized Mylar with a thickness of 6 μm for the other two – and covered only by a 100- $\mu\text{g}/\text{cm}^2$ acrylic film. The source-holder geometry is shown in Fig. 2.

All three of these radioactive sources emit γ rays as well as electrons and, although our thin scintillator is relatively insensitive to the former, we nonetheless took extra precautions to ensure that we were only studying the detector’s response to the latter. In addition to recording a spectrum from each source as already described, we also recorded a second spectrum with a 2-mm-thick aluminum plate inserted between the source and the detector. This plate was thick enough to remove all the β particles without significantly attenuating the γ rays. We then subtracted this second spectrum from the first, and considered the resultant spectrum to be a “pure” β spectrum. This method has one flaw, however: the spectrum obtained with the aluminum plate includes some contribution from the bremsstrahlung created by the β particles as they stop. Thus, we took the same approach with the calculated Monte Carlo spectra: we made two calculations for each source, one with an aluminum plate and one without, took the difference between them and then compared that difference spectrum with the “pure” experimental β spectrum.

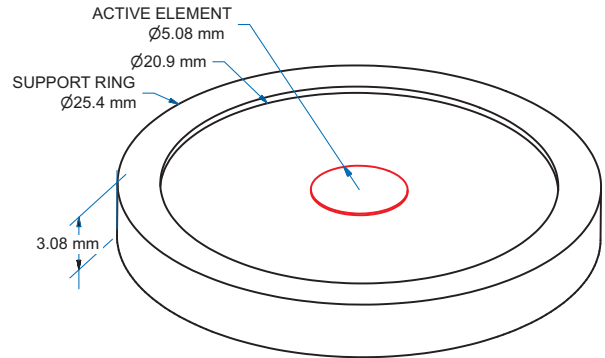


Fig. 2. Radioactive-source geometry: the support ring is made from aluminum.

3. Geant4 Physics Model

The Geant4 Simulation Toolkit includes a series of packages for the simulation of electromagnetic interactions of particles with matter, specialized for different particle types, energy range and specific physics model. In our work, we considered only electrons, γ rays and x rays, and used three different physics models for the electromagnetic (EM) processes: the *standard* EM package, the *low-energy* EM package and the *Penelope* EM package. In all cases, fluorescence emission, Rayleigh scattering and Auger interactions were included in the EM physics model where appropriate. The *standard* EM package is based on an analytical approach [11,12,13]; its effective energy range is nominally between 1 keV and 100 TeV but it neglects atomic effects and is mainly used in high-energy physics applications. The *low-energy* package is optimized for our energy region and extends the range of validity for electrons and photons down to 250 eV [7,8] and even below. The *Penelope* package is an alternative low-energy implementation; it is a re-engineered version [14] of the original PENELOPE Monte Carlo code [15,16]. Detailed information on these packages, as well as on the design of the Geant4 toolkit can be found in Ref. [3] and in the Physical Reference Manual of Geant4 [17] and references therein.

The validation of the Geant4 electromagnetic physical processes is important in order to reach an adequate level of precision in applications such as ours. Systematic and extensive validation is an on-going process in the Geant4 collaboration and recently microscopic quantities such as cross sections, angular/energy distributions, attenuation coefficients, stopping powers and ranges have also been examined in a systematic way [18], and their

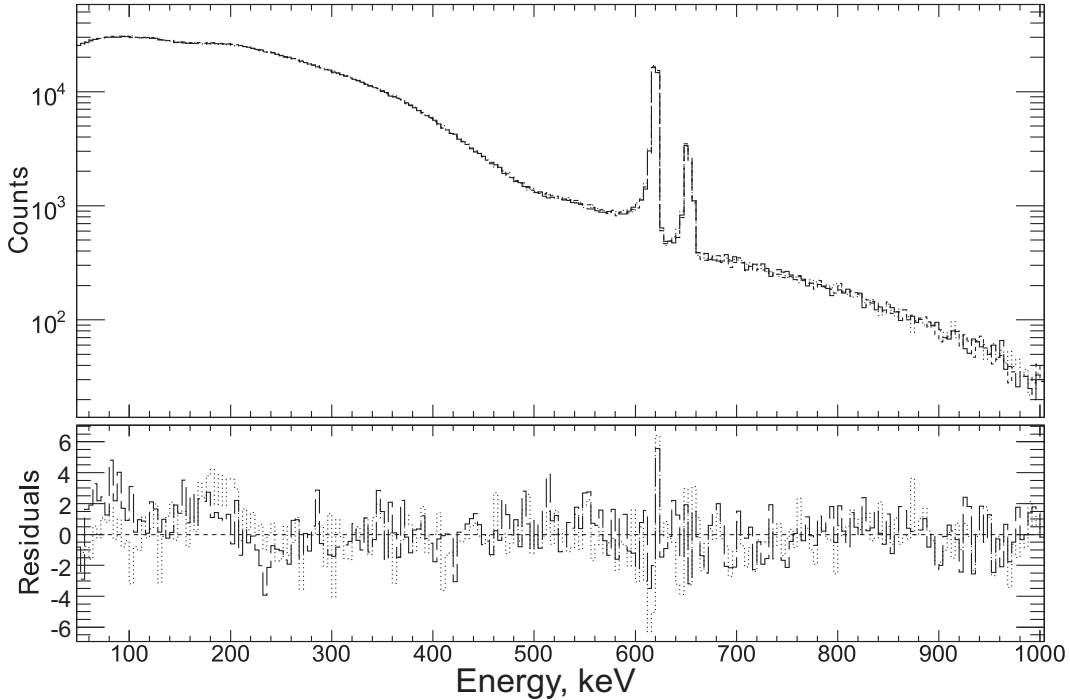


Fig. 3. Upper panel: Energy deposition in the β -detector as generated by Geant4 Monte Carlo calculations for the decay of ^{137}Cs . Three different EM physics models are used and all three are plotted although they are so similar that they cannot be distinguished. Lower panel: To clarify the differences among the results for the three EM physics models, the *low-energy* EM package is used as our standard, and differences between each of the other two models and the *low-energy* package are plotted as residuals in standard-deviation units. The dashed line corresponds to the *Penelope* EM package (compared with the *low-energy* package); while the dotted line corresponds to the *standard* EM package (also compared with the *low-energy* package).

compatibility with reference data from the U.S. National Institute of Standards and Technologies (NIST) has been established [14].

Here we have restricted ourselves to a comparison between Geant4 calculations and experiment for the energy deposited by electrons in a thin plastic scintillator, where we have used the very simple laboratory geometry already described so that the Monte Carlo geometry could reproduce it exactly. As can be seen in the top panel of Figure 3, under these conditions the three physics models – *standard* EM, *low-energy* EM and *Penelope* EM – generate energy spectra that differ very little from one to another. The bottom panel of the figure shows the normalized residuals between the first and second models, and between the second and third ones: there are small but perceptible differences below 200 keV but nothing significant above that energy. We also compared the total β -efficiencies obtained from the three EM physics models. Including all energies between 50 and 1000 keV, the calculated Monte Carlo efficiencies were 15.16(3)%, 15.18(3)%, and 15.11(3)%, respectively. If the low-energy thresh-

hold was increased to 75 keV the calculated efficiencies were 13.79(3)%, 13.84(3)% and 13.82(3)%. For both thresholds the three physics models yielded statistically identical results. In short, for our purposes we find nothing in these results to choose between the three available physics models.

Even so, we chose to use the *low-energy* EM model in all the Monte Carlo simulations presented in the remainder of this paper. Although it took considerably more computer time per calculation than did the standard EM model, we considered that it was, in principle, more appropriate to our energy region since it was specifically designed for better performance at low energies. A detailed inter-comparison of results from the three physics models for the total efficiency of the plastic β -detector as a function of β energy will appear in a subsequent publication [19].

4. Geant4 Geometry

In defining the laboratory geometry in Geant4 we included all the components of the detector assembly and source housing (see Figs. 1 and 2, and Ta-

Table 2

Composition of the different materials used in the Monte Carlo simulations performed in this work. The tabulated values correspond to the element mass fraction in each material, given in percentages. Material densities are also given.

Chemical element	Air	Acrylic	Mylar	Havar	Stainless Steel	PVC	Lucite	BC404	Aluminum
H		0.71	4.20			4.84	8.07	8.45	
C	0.01	8.52	62.50	0.04		38.44	59.97	91.55	
N	75.53	90.77							
O	23.18		33.30				31.96		
Ar	1.28								
Be				0.01					
Cl						56.73			
Si					1.00				
Cr				17.04	19.00				
Ni				12.50	10.00				
Fe				16.34	68.00				
Co				41.04					
Mo				3.14					
Mn				1.45	2.00				
Al									100.00
W				8.44					
Density g/cm ³	0.0012	1.190	1.390	8.300	8.020	1.380	1.185	1.032	2.700

ble 1), with everything placed in air. Special care was taken to include all components of the various materials, with the natural isotopic abundances for each element properly accounted for. Table 2 lists the composition and density of all materials used in the Geant4 calculations.

As explained in Section 2, two Monte Carlo simulations were performed for each source, one with a 2-mm-thick plate of aluminum located between the source and the detector, and one without it. The spectrum we plot for each source is the difference between these two spectra. In defining the geometry in Geant4 we incorporated a plate and chose its material to be either aluminum or air, depending on the desired effect. Fig. 4 shows the tracks of electrons for both types of simulations.

5. Geant4 Parameter Control

Geant4 allows the user to define different regions in the experimental setup, and to set a different particle-production threshold in each one [9]. This capability allows for simulation accuracy and speed optimization according to the needs of a particular experiment. We defined three regions: the radioactive source, the thin plastic scintillator and everything else. In the first two, the threshold for produc-

ing secondary particles was kept very low in order to simulate all physics interactions as well as possible; in the third, a much higher production threshold was chosen. This approach considerably reduced the computing time without compromising the results. A test run with low thresholds in all regions did not reveal any significant differences from the sped-up version with different thresholds in different regions.

It was pointed out by Kraev [20] that, to get good agreement with experiment, it is important to choose two parameters particularly carefully in the *low-energy* EM physics model of Geant4: the cut for secondaries (*CFS*) value, which determines the production threshold for secondary particles, and the f_r -parameter, which limits the step size for tracking β -particles at a material boundary. In this work, we used $CFS = 10 \mu\text{m}$, which is recommended as an acceptable compromise between a “good” description of the scattering processes and a reasonable computation time. For the f_r -parameter we used 0.02 as recommended in [20]; this is actually the default value for the Geant4 version 4.9.0.

6. Comparison with Experiment

To simulate the decay of a radioactive nuclide with Geant4, it is possible to define each γ transi-

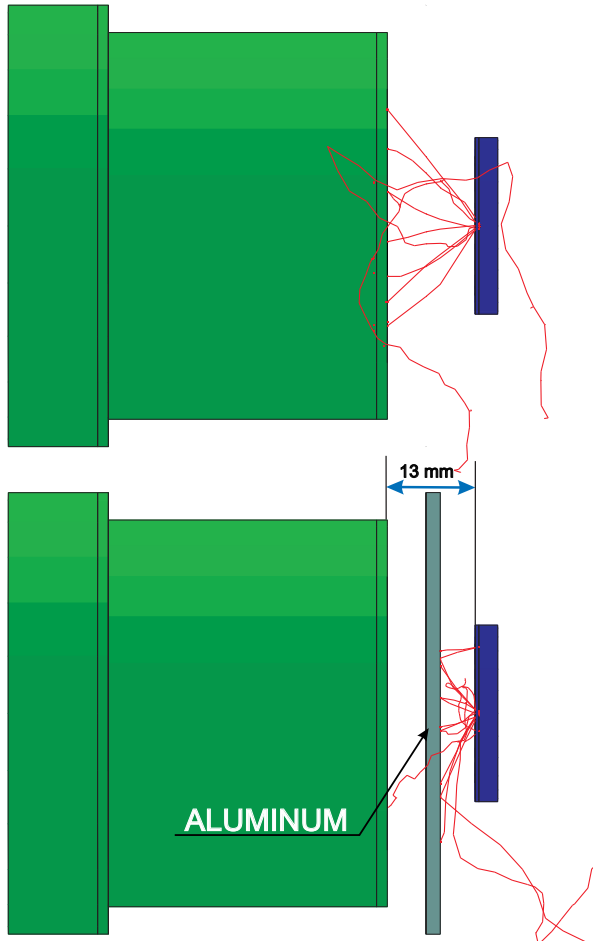


Fig. 4. Schematic view of the geometry arrangements for Monte Carlo simulations, showing sample electron trajectories. The upper panel shows trajectories when there is only air between the source holder (right) and the detector housing (left). The lower panel shows them when a 2-mm-thick aluminum plate is introduced.

tion, internal-conversion line and β -decay spectrum individually and require Geant4 to transport all particles through the specified materials and determine the spectrum in the scintillator. However, the code also offers a radioactive-decay module, which generates all the decay components radiated from a specified source using information extracted from the Evaluated Nuclear Structure Data File (ENSDF) [21].

To generate the Monte Carlo emission spectra we began by programming Geant4 based on the radioactive-decay module. The primary electron spectrum emitted from ^{207}Bi generated with the radioactive-decay module is shown in Fig. 5. When repeating this procedure for ^{133}Ba , to our surprise we found that the electron emission spec-

trum produced by the radioactive-decay module of Geant4 was simply not correct, yielding relative conversion-electron intensities in significant disagreement with ENSDF data. The emission spectrum from ^{137}Cs also turned out to be incorrect, but here the main problem was more subtle: there are two β -decay branches from ^{137}Cs , which are both treated by Geant4 as allowed. In fact both transitions are forbidden, with shape-correction factors that have been determined by Behrens and Christmas [22] from experimental data. In addition, the radioactive-decay module gives the incorrect intensity for one of the conversion electron lines of ^{137}Cs ($I_{655.7\text{ keV}}=1.10\%$ instead of 1.39%). In both these decays – of ^{133}Ba and ^{137}Cs – we bypassed the radioactive-decay module and inserted each decay mode and transition individually, with the correct intensities for the conversion electrons and the correct shape for the forbidden β transitions. For these we used the General Particle Source module available in the Geant4 [23], which allows the user to define standard energy, angle and space distributions of the primary particle.

Based on a primary spectrum thus generated for each source, the Monte Carlo code then determined the total energy deposited in the scintillator. However, before this result could be compared with the experimental spectrum, it was necessary to add the effects of statistical fluctuations introduced by the processes of light production and transmission, as well as photomultiplication and electronic pulse analysis. For this purpose, we looked to a published study of the response of a plastic scintillator to mono-energetic beams of positrons and electrons

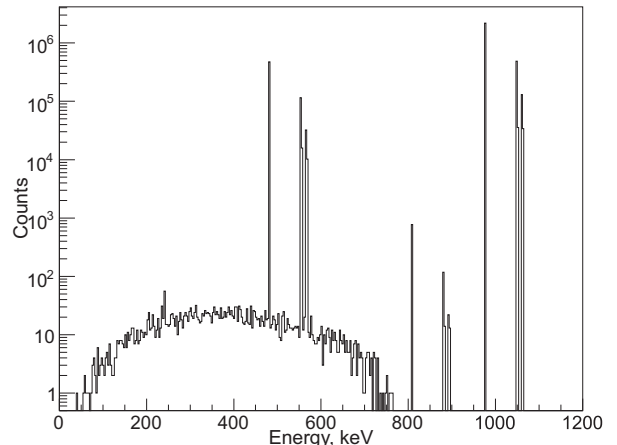


Fig. 5. Decay spectrum for ^{207}Bi generated by Geant4 with its internal radioactive-decay module activated. Only electrons are shown.

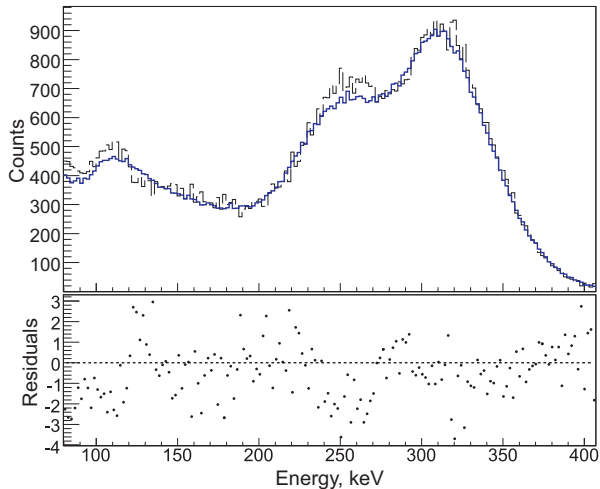


Fig. 6. In the top panel, the measured spectrum (thick solid line) for the decay of ^{133}Ba is compared with the Geant4-simulated result (thin dashed line). The *low-energy* EM package was used. Residuals in standard-deviation units are plotted in the lower panel. The reduced χ^2 in the energy range 80 – 406 keV is 0.4.

[24], which tabulated the width of the full-energy Gaussian peak as a function of energy between 0.8 and 3.8 MeV. Since we also needed to deal with energies lower than that, we took the width to be linearly dependent on energies below 0.8 MeV.

Our procedure was to take the scintillator spectrum produced by Geant4 and process it by a randomization algorithm written in C++ in the ROOT [25] analysis framework. In essence, this process spread the number of counts in each energy bin into a Gaussian distribution centered at the original energy and with a width, σ , taken or extrapolated from Ref. [24]. The results could then be compared directly with the measured spectra.

The measured spectra for all three sources were taken under exactly the same conditions. A description of the data acquisition system used in these measurements is given in ref. [4] and references therein. The amplifier gain, photomultiplier high voltage, and low-energy electronic threshold remained unchanged for all three sources. The threshold was chosen to be identical to the setting used during our branching-ratio measurements of super-allowed Fermi β -decays. (This hardware threshold was higher than the software threshold.) This ensured that the results of our comparisons between source measurements and Monte Carlo simulations could be readily applied to our accelerator-based measurements.

In comparing our measured spectra with Monte Carlo results, we the slope of the energy calibra-

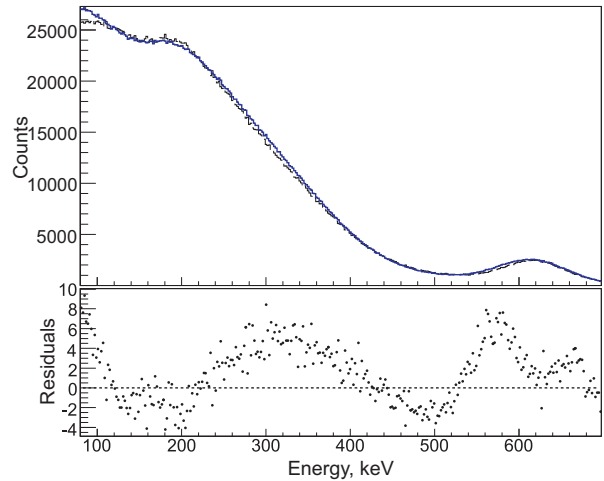


Fig. 7. In the top panel, the measured spectrum (thick solid line) for the decay of ^{137}Cs is compared with the Geant4-simulated result (thin dashed line). The *low-energy* EM package was used. Residuals in standard-deviation units are plotted in the lower panel. The reduced χ^2 in the energy range 80 – 697 keV is 4.0.

tion (*i.e.* the energy per channel) and its offset (*i.e.* the zero-energy channel) corresponding to each measured spectrum as adjustable fit parameters, which were used to optimize the agreement with the Monte Carlo spectrum. We wrote our own C++ ROOT program to accomplish this purpose. The resulting comparisons for our three sources, as well as the normalized residuals, for ^{133}Ba , ^{137}Cs and ^{207}Bi , appear in Figures 6, 7 and 8 respectively.

The agreement between the Geant4 Monte Carlo simulations and experiment is good for all three sources considered in this work, ^{133}Ba , ^{137}Cs and ^{207}Bi , although for the latter one the normalized χ^2 of 8.9 is less impressive than for other two. In that case, the energy range, which extended from 80 to 1143 keV, was much greater than for the other too. This may be partly responsible for the higher χ^2 but another possibility is that our simple linear extrapolation of the results in Ref. [24] does not fully describe our system’s response function at low energies. If in fact the peak resolution were somewhat worse than this extrapolation indicates – a not unreasonable possibility – then the agreement with experiment would be considerably improved. It is also worth noting that the slight non-alignment in peak positions, which is evident in all three spectra, can be explained by possible small non-linearities in the experimental energy response.

Since the amplifier gain and photomultiplier high voltage were kept the same for all three measurements, the fitted slopes and offsets obtained for all

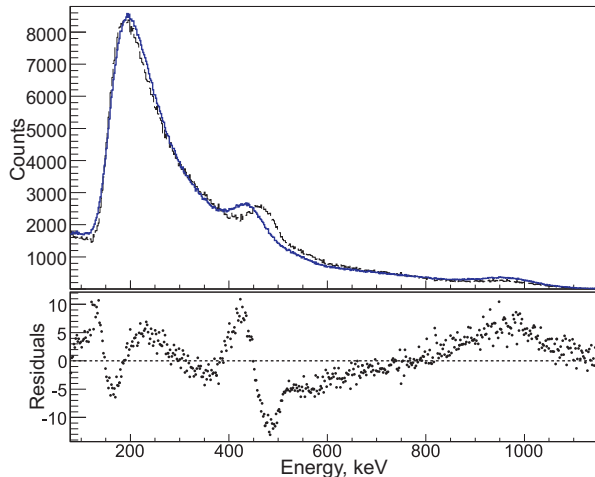


Fig. 8. In the top panel, the measured spectrum (thick solid line) for the decay of ^{207}Bi is compared with the Geant4-simulated result (thin dashed line). The *low-energy* EM package was used. Residuals in standard-deviation units are plotted in the lower panel. The reduced χ^2 in the energy range 80 – 1143 keV is 8.9.

three spectra should have been very nearly the same. In fact they were, but, as a quantitative measure of consistency, we took the average values for the slope and offset, and again evaluated the normalized χ^2 for the comparison between experiment and simulation. The new values for the normalized χ^2 were, of course, somewhat increased, being 3.6, 9.5, and 16.3 for ^{133}Ba , ^{207}Bi , and ^{137}Cs , respectively, but the agreement is still quite satisfactory. Most crucially for our purposes, the low-energy thresholds in all three cases were in close agreement, with 80 ± 3 keV being the common value.

As stated in the introduction, the result of the simulation that matters most to us is how well it reproduces the fraction of the total β spectrum that lies above some low-energy threshold, typically around 80 keV. The spectral details at higher energy are only important to us to the extent that they change the fraction of counts recorded above threshold. The fact that the fits performed with the low-energy threshold as a free parameter give the same result for all three isotopes, serves as important assurance that the fitted threshold value is consistent with the actual one.

Although the activity of the radioactive sources that we used for this work are nominally $1 \mu\text{Ci}$ (37-kBq), the accuracy of this value was only quoted to and approximate $\pm 15\%$ by the supplier. So that we could get a more precise value for our β -detector efficiency, we made our own measurement of the ^{207}Bi source activity using a well-calibrated HPGe

γ -detector [27] to detect the known γ rays from the decay. In this way we established the source activity to be $1.31(1) \mu\text{Ci}$ at 16 January, 2008. Now, knowing the activity of the source as well as the low-energy detection threshold already obtained from our fit, we could deduce from our experimental data the absolute efficiency of the β -detector to be $3.48(2)\%$ at the distance of $13.2(1)$ mm. With exactly this geometry, the Geant4 simulation yielded an absolute efficiency of $3.50(1)\%$, in excellent agreement with experiment.

7. Conclusion

The electron spectra we have obtained from Monte Carlo simulations are generally in good agreement with experimental data. All identifiable features that are present in the experimental spectra are reproduced in the simulated ones, and in most cases their relative intensities agree as well. Furthermore, the threshold energy and absolute efficiency are well reproduced. Our results clearly demonstrate that Geant4 version 4.9.0 can be used effectively to simulate the β -spectra as measured by our thin plastic scintillator detector.

In particular for our application, where we need only rely on the simulation to determine the energy dependence of the β -detector's total efficiency with a low-energy threshold at ~ 80 keV, it is clear that Geant4 will provide the precision we require.

However, we have also shown that the radioactive-decay module included in Geant4 to simulate the initial radiation from a radioactive source should only be used with care: it is essential to check its output carefully. In particular, the intensities of conversion-electron lines produced by this module were sometimes found to be incorrect and, if any forbidden β -decay branches are involved, their spectrum shapes may not be correctly generated.

References

- [1] J. C. Hardy and I. S. Towner, Phys. Rev. C 71 (2005) 055501.
- [2] I. S. Towner and J. C. Hardy, Phys. Rev. C 77, (2008) 025501.
- [3] S. Agostinelliae *et al.*, Nucl. Instr. and Meth. A 506 (2003) 250, and Geant4 Home Page, <http://geant4.cern.ch/>.
- [4] V. E. Iacob *et al.*, Phys. Rev. C 74 (2006) 015501.
- [5] J. C. Hardy *et al.*, Phys. Rev. Lett. 91 (2003) 082501.

- [6] R. G. Helmer *et al.*, Nucl. Instr. and Meth. A 511 (2003) 360.
- [7] J. Apostolakis *et al.*, CERN-OPEN-034 (1999).
- [8] S. Chauvie *et al.*, in: Nuclear Science Symposium Conference Record, 2004 IEEE, Vol. 3, (2004) 1881.
- [9] J. Allison *et al.*, IEEE Trans. Nucl. Sci. 53 (2006) 270.
- [10] AccuRange 600™ Laser Displacement Sensor Home Page, <http://www.acuitylaser.com/AR600/sensor-technical-data.shtml>.
- [11] K. Amako *et al.*, Nucl. Phys. B, Proc. Suppl. 150 (2006) 44.
- [12] H. Burkhardt *et al.*, in: Nuclear Science Symposium Conference Record, 2004 IEEE, Vol. 3, (2004) 1907.
- [13] V. Ivanchenko *et al.*, in: Proceedings of the CHEP'04, CERN 2005-002 Vol. 1, (2005) 207.
- [14] K. Amako *et al.*, IEEE Trans. Nucl. Sci. 52 (2005) 910.
- [15] J. Baro *et al.*, Nucl. Instr. and Meth. B 100 (1995) 31.
- [16] J. Sempau *et al.*, Nucl. Instr. and Meth. B 207 (2003) 107.
- [17] Geant4 Colaboration, Physics Reference Manual, CERN (2007), <http://geant4.cern.ch/support/userdocuments.shtml>.
- [18] G. Cirrone *et al.*, in: Nuclear Science Symposium Conference Record, 2003 IEEE, Vol. 1, (2003) 482.
- [19] V.V. Golovko *et al.*, to be published.
- [20] I. S. Kraev, Ph.D. thesis, KU Leuven (2006).
- [21] J. Tuli, Brookhaven National Lab report, BNL-NCS-51655-02-Rev (2001).
- [22] H. Behrens and P. Christmas, Nucl. Phys. A399 (1983) 1310.
- [23] General Particle Source Home Page, <http://reat.space.qinetiq.com/gps/>.
- [24] E. T. H. Clifford *et al.*, Nucl. Instr. and Meth. 224 (1984) 440.
- [25] R. Brun and F. Rademakers, Nucl. Instr. and Meth. A 389 (1997) 81.
- [26] Ortec TRUMP Home Page, <http://www.ortec-online.com/trump.htm>.
- [27] J. C. Hardy *et al.*, Appl. Rad. and Isotopes 56(1-2) (2002) 65-69.